Astronomy & Astrophysics manuscript no. ngc6357
June 11, 2014
© ESO 2014

Probing embedded star clusters in the HII complex NGC 6357 with VVV⋆

E. F. Lima,[1,2] E. Bica,[1] C. Bonatto[1] and R. K. Saito[3]

[1] Universidade Federal do Rio Grande do Sul, Departamento de Astronomia
CP 15051, Porto Alegre 91501-970, Brazil
e-mail: eliade.lima@ufrgs.br, bica@if.ufrgs.br, charles@if.ufrgs.br

[2] Departamento de Física, CCNE, Universidade Federal de Santa Maria
97105-900, Santa Maria, RS, Brazil

[3] Departamento de Física, Universidade Federal de Sergipe
Av. Marechal Rondon s/n, 49100-000, S£o Cristóvão, Brazil

Received xxxxxxx; accepted xxxxxx

ABSTRACT

Context. NGC 6357 is an active star-forming region located in the Sagittarius arm displaying several star clusters, which makes it a very interesting target to investigate star formation and early cluster evolution.
Aims. We explore NGC 6357 with the "VISTA Variables in the Vía Láctea" (VVV) photometry of seven embedded clusters (ECs), and one open cluster (OC) projected in the outskirts of the complex.
Methods. Photometric and structural properties (age, reddening, distance, core and total radii) of the star clusters are derived. VVV saturated stars are replaced by their 2MASS counterparts. Field-decontaminated VVV photometry is used to analyse Colour-Magnitude Diagrams (CMDs), stellar radial density profiles (RDPs) and determine astrophysical parameters.
Results. We report the discovery of four ECs and one intermediate-age cluster in the complex area. We derive a revised distance estimate for NGC 6357 of 1.78 ± 0.1 kpc based on the cluster CMD morphologies. Among the ECs, one contains the binary star the WR 93, while the remaining ones are dominated by pre-main sequence (PMS) stars, young-stellar objects (YSO) and/or and have a developed main sequence. These features reflect a significant age spread among the clusters. Evidence is found that the relatively populous cluster Pismis 24 hosts two subclusters.

Key words. (Galaxy): open clusters and associations: general – (Galaxy): open clusters and associations: individual: NGC 6357 – Infrared: stars – surveys

arXiv:1406.2413v1 [astro-ph.SR] 10 Jun 2014

1. Introduction

Star-forming complexes are, in general, major building blocks of the large-scale structure of galaxies and important sites to study how massive stars form (Russeil et al. 2010). In particular, Galactic embedded and open clusters are excellent probes of the structure and evolution of the disk and spiral arms (Carvalho et al. 2008; Lada & Lada 2003; Friel 1995). Embedded clusters (ECs) can be partially or fully immersed in embryonic molecular clouds and HII regions. According to Leisawitz et al. (1989), all clusters younger than ∼ 5 Myr are connected at least to one large molecular cloud or HII region.

Recently, our group studied the stellar content of the Sh2–132 HII region, a star-forming complex hosting at least 4 ECs and presenting evidence of triggered star formation and hierarchical structuring (Saurin et al. 2010). Sequential star formation in giant molecular clouds was also studied by Camargo et al. (2011). Observationally, low-mass star clusters younger than about 10 Myr present an underpopulated, developing main sequence (MS) and a more populous feature of pre-main sequence (PMS) stars (Bonatto & Bica 2009a). Studies of very young star clusters hosting PMS and MS stars have produced well-defined CMDs, RDPs and mass functions (Bonatto & Bica 2009c). Recently additional tools were developed by our group allowing to obtain reliable fundamental parameters of early–cluster phases (Bonatto et al. 2012a,b). The present paper focuses on the ECs in the NGC 6357 complex.

NGC 6357 (≡ W 22 ≡ RCW 131 ≡ Sh2–11) is a large HII region complex that consists of a shell of about 60×40 arcmin^2, bright optical nebulosities in different evolutionary stages, OB stars belonging to the populous open cluster Pismis 24 and YSOs candidates (Felli et al. 1990; Bohigas et al. 2004; Wang et al. 2007; Russeil et al. 2010; Fang et al. 2012). Persi et al. (1986) showed that the whole HII complex is an active area of recent and on-going star formation. The shell has been interpreted as an ionized gas bubble created by the strong winds of the current massive stars in Pismis 24 or by a previous generation (Lortet et al. 1984; Bohigas et al. 2004; Wang et al. 2007). The total amount of molecular gas related to the large shell was estimated by Cappa et al. (2011) as 1.4×10^5 M$_\odot$.

Early optical studies of NGC 6357 and Pismis 24 revealed ∼20 O-type and early B-type stars (Moffat & Vogt 1973; Neckel 1978, 1984; Lortet et al. 1984), including a binary system

⋆ Based on observations taken with the ESO VISTA Public Survey VVV, Programme ID 179.B-2002 and data from the 2MASS VizieR Catalog II/246.

(HD 157504) composed of a WC7 Wolf-Rayet star (WR 93) and an O7-9 star (van der Hucht 2001). Two of the cluster members, namely Pismis 24-1 (HDE 319718) and Pismis 24-17, were recently classified as spectral type O3.5, some of the brightest and bluest stars known (Massey et al. 2001; Walborn et al. 2002). The total to selective extinction ratio (R_V) towards NGC 6357 appears to be about 3.5 (Russeil et al. 2012; Bohigas et al. 2004).

A wide range of distances (1.1 – 2.6 kpc) has been derived to NGC 6357. This is usually estimated from the distance of Pismis 24. The most recent determination is that of Fang et al. (2012), who give 1.7±0.2 kpc. The kinematic distance is $d_\odot$=1.0±2.3 kpc (Wilson et al. 1970). Neckel (1978) obtain $d_\odot$=1.74±0.31 kpc and Massey et al. (2001) find a distance of 2.56±0.10 kpc for Pismis 24. Conti & Vacca (1990) and van der Hucht (2001) derived for WR 93 $d_\odot$=1.1 kpc and $d_\odot$=1.74 kpc, respectively.

Optical, radio continuum, and near- and mid-IR images of NGC 6357 (Cappa et al. 2011) indicate the giant nature of this complex and its evolved character, which suggest a suitable laboratory for early dynamical and hydrodynamical evolution. The number of ECs in a given star-forming region is fundamental to study the gas expulsion and dynamical evolution effects (Carvalho et al. 2008). Using the recent VVV JHK$_S$ data (Minniti et al. 2010), we analyse in detail in the present paper the stellar clusters detected in NGC 6357. We employ a field-decontamination algorithm (Bonatto & Bica 2007b) adapted to VVV photometry to analyse CMDs, RDPs and determine the astrophysical parameters. The present analysis of the ECs shows structural variations as well as morphology diversity of MS and PMS evolutionary sequences in CMDs. Based on this, we infer the star formation history in the complex.

This paper is organised as follows. In Sect. 2 the stellar cluster sample is described. In Sect. 3 we provide details on the VVV data adopted. In Sects. 4 and 5, the cluster photometric and structural analyses are carried out. In Sect. 6 we discuss the results and give conclusions.

2. Stellar clusters in NGC 6357

Several studies on NGC 6357 are available in the literature, in particular on the cluster Pismis 24. The WEBDA[1] database locates the center of Pismis 24 at $\alpha(2000)=17^h25^m32^s$ and $\delta(2000)=-34°25'00''$, and provides a distance from the Sun $d_\odot$ ~1.99 kpc, reddening E(B-V)=1.72, and age of 10 Myr. WR 93 has been considered a member of Pismis 24 (Massey et al. 2001). However, this star is located 4′ away from the cluster center. We investigate further this issue.

To the southeast ($\alpha(2000)=17^h25^m32^s$ and $\delta(2000)=-34°24'20''$) of the complex is located an object first reported as ESO392-SC11 (Lauberts 1982). It has been as well reported as AH03 J1725-34.4 (Archinal & Hynes 2003), BDS 100 (Bica et al. 2003), G351.1+0.7 cluster (Damke et al. 2006), and is also indicated in Moisés et al. (2011). This extended (~3.5′) overdensity appears to be related to the general young population of the complex. It is classified as a star cluster, see e.g. the DAML02 database[2] (Dias et al. 2002). They employed the designation AH03 J1725-34.4 and show an apparent diameter of 2.6′, a distance of 290 pc (too short for NGC 6357 complex) and an age of 7 Myr. In the present paper we use VVV data to constrain not only parameters, but the nature itself of this object as a young stellar cluster or an OB association (Sect. 4.4). In the present study we also focus our attention on the compact cluster BDS 101 (Table 1) found by Bica et al. (2003), which is located at ~1′ NW of the center of ESO392-SC11.

We show in Table 1 the star clusters analysed in this work. Four star clusters were discovered by two of us (E. L. and E. B.). They are given VVV cluster identifications, in continuation to the recent cluster numbering by Borissova et al. (2014). They span the interval VVV CL164 to VVV CL167, according to the VVV designations.

In Fig. 1 we show the angular distribution of the studied objects on a DSS image of the nebular complex NGC 6357. We can identify the presence of the stellar clusters in shell-like features from Cappa et al. (2011). Pismis 24 (together with VVV CL165 and VVV CL166) is located near the border of G353.12+0.86. VVV CL167 might be related to a ring nebula. Finally, BDS 101 and ESO 392-SC 11 are located in G353.1+0.6.

In Fig. 2 we show a VVV JHK_s blow up image of three embedded clusters and one open cluster in the sample. We emphasize the difference between embedded and open stellar clusters, the former are embedded in parental molecular clouds and the stellar content is in general dominated by PMS stars (e.g. Lada & Lada 2003; Bonatto et al. 2006b). On the other hand, OCs are dynamical survivours of the embedded phase (Bastian & Goodwin 2006). Pismis 24 has very massive stars in the central region and attached to the North is the bright dust/HII region G353.2+0.9 (Cappa et al. 2011). BDS101 is a compact EC while the loose one VVV CL167 is older. VVV CL164 is an OC projected in the NGC 6357 area (Sect. 4.2.4).

3. VVV photometry and data

VVV is an ESO Public Survey scanning the Galactic bulge and plane with the 4-m class VISTA Telescope at Paranal (Minniti et al. 2010). The total observed area is about 562 deg^2, scanning -10.0°$\lesssim b \lesssim$ +10.5° and -10.3°$\lesssim l \lesssim$ +5.1° in the bulge, and within 294.7°$\lesssim l \lesssim$ 350.0° and -2.25°$\lesssim b \lesssim$ +2.25° in the plane. The VVV survey observes in five passbands, namely Z (0.87 μm), Y (1.02 μm), J (1.25 μm), H (1.64 μm), and K_S (2.14 μm). It also conducts a variability campaign in the K_S-band only, with ~100 pointings spanning six years (20102016). The JHK$_S$ observations were completed during the first semester of 2011. The present work is based on J, H and K$_S$ photometry, from the VVV Data Release 1 (DR1) (Saito et al. 2012).

Each unit of VISTA observations is called a tile, consisting of six individual pointings (or "pawprints") and covers a 1.64 deg^2 field of view. To fill up the VVV area, a total of 348 tiles are used, with 196 covering the bulge (a 14×14 grid) and 152 the Galactic plane (a 4 × 38 grid). The NGC 6357 complex appears in the VVV bulge/disk tiles b329 and b343.

Photometric catalogues for the VVV images are provided by the Cambridge Astronomical Survey Unit (CASU)[3]. The catalogues contain the positions, magnitudes, and some shape measurements obtained from different apertures, with a flag indicating the most probable morphological classification. The limiting magnitude for the aperture photometry of the catalogues occurs at K$_S$=18 mag in most disk fields. The VVV data are in the natural VISTA Vegamag system, with the photometric calibrations in JHK_S performed using the VISTA magnitudes of unsaturated 2MASS[4] stars present in the images. The present work is based on the derived colours and magnitudes established by

[1] http://www.univie.ac.at/webda/webda.html

[2] http://www.astro.iag.usp.br/ocdb/file/clusters.txt

[3] http://casu.ast.cam.ac.uk/vistasp/

[4] The Two Micron All Sky Survey, All Sky data release (Skrutskie et al. 2006)

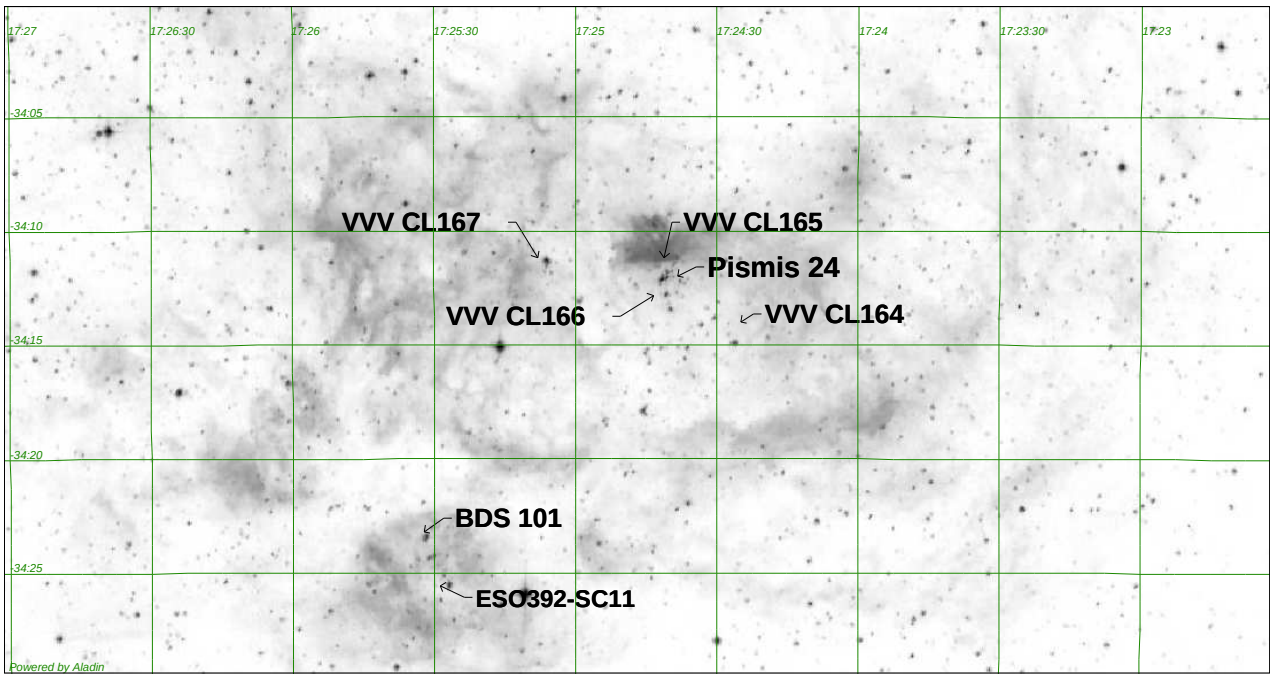

Fig. 1. 55′ × 30′ DSS R image of the emission nebula NGC 6357. We indicate the present sample of star clusters.

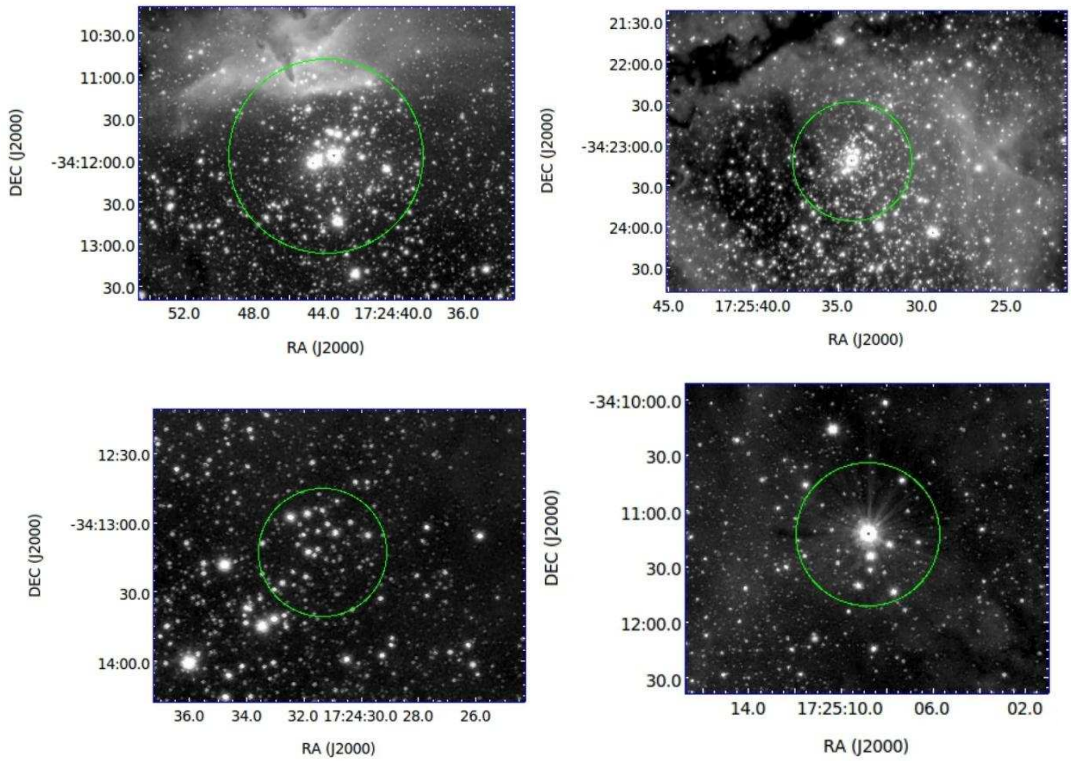

Fig. 2. Combined JHK$_S$ VVV images of clusters in the nebula NGC 6357. Top panels: Pismis 24 (left), BDS 101 (right). Bottom panels: newly found clusters VVV CL164 (left) and VVV CL167 (right). The circles indicate the angular sizes of the clusters (Table 1).

the CASU v1.3 pipeline reduction. The detailed account of the CASU pipeline can be found in Irwin et al. (2004).

Only sources with VVV K$_S$ photometry defined as stellar (sources with a Gaussian sigma parameter between 0.9 and 2.2) were selected. Saturated stars in the VVV data, usually brighter than J, H and K$_S$ ∼11 mag, were replaced by the respective 2MASS magnitudes.

Table 1. Star clusters towards NGC 6357.

Cluster	α (J200)	δ (J200)	l (°)	b (°)	R (arcmin)	Comments
(1)	(2)	(3)	(4)	(5)	(6)	(7)
Pismis 24[a]	17:24:44	-34:11:56	353.17	0.89	1.5	optical EC
BDS 101[b]	17:25:34	-34:23:09	353.11	0.65	0.7	infrared EC
ESO 392-SC 11[c]	17:25:32	-34:24:20	353.09	0.64	1.7	EC or OB association?
VVV CL164[d]	17:24:31	-34:13:15	353.12	0.92	0.5	infrared OC
VVV CL165[d]	17:24:45	-34:11:28	353.18	0.89	0.2	subcluster of Pismis 24?
VVV CL166[d]	17:24:47	-34:12:36	353.17	0.88	0.2	subcluster of Pismis 24?
VVV CL167[d]	17:25:09	-34:11:13	353.23	0.83	0.6	infrared EC surrounding WR 93

Notes. Cols. 2 to 5: Optimised central coordinates. Col. 6: The radii were set by eye for decontamination purposes (Sect. 4.1). [(a)] Moffat & Vogt (1973) [(b)] Bica et al. (2003). [(c)] Sect. 2 [(d)] Discovered in the present paper.

4. Star cluster analyses

Besides analysing open clusters (e.g. Bonatto & Bica 2009a), our group has also concentred efforts to study in detail embedded clusters, by developing tools to extract information from the CMDs and RDPs (e.g. Bonatto & Bica 2009c, 2010).

NGC 6357 in itself is an astrophysical laboratory, not only for its numerous interstellar structures, e. g. filaments, bubbles, knots, etc, but also for its ECs (Table 1). VVV photometry provides an adequate means to explore them, in such a crowded fields towards the central disk and bulge.

4.1. Field star decontamination

Field-star decontamination is usually required for the identification and characterisation of star clusters. To disentangle field and cluster stars we use a statistical decontamination algorithm (Bonatto & Bica 2007a, 2010) adapted to the photometric depth of VVV. The comparison fields used for the decontamination depend on the projected distribution of individual stars and the presence of other clusters and/or clumpy extinction due to dark clouds in the area. Examples are a ring around the cluster or some other comparison field selected in its vicinity. The algorithm measures the relative number densities of probable field and cluster stars in cubic CMD cells with axes along the J magnitude and (J-H) and (J-K_S) colours. It (i) divides the range of CMD magnitude and colours into a 3D grid, (ii) estimates the number density of field stars in each cell based on the number of comparison field stars with similar magnitude and colours as those in the cell, and (iii) subtracts the expected number of field stars from each cell. Input algorithm parameters are the cell dimensions ΔJ=1.0 and Δ(J-H)=Δ(J-K_S)=0.2 mag. Summing over all cells, each grid setup produces a total number of member stars $\langle N_{mem} \rangle$ and, repeating this procedure for the 729 different setups (different cell sizes and their positionings), we obtain the average number of members $\langle N_{mem} \rangle$. Each star is ranked according to the number of times they survive all runs (survival frequency) and only the $\langle N_{mem} \rangle$ highest ranked stars are accepted as cluster members and transposed to the respective decontaminated CMD.

We decontaminated CMDs to investigate the nature of star cluster candidates and derive their astrophysical parameters. In summary, we applied (i) field-star decontamination to uncover the intrinsic CMD morphology, essential for derivation of reddening, age, and distance to the Sun, and (ii) colour-magnitude (CM) filters (Fig. 3) to exclude stars unlike those of the CMD sequence. The latter filters are wide enough to include cluster MS and PMS stars, together with the photometric uncertainties and binary star effects (Sect. 4.2). In the following sections we will make use of this tool several times in the analyses. The latter procedure is required for intrinsic stellar RDPs. In particular, the use of field-star decontamination in the construction of CMDs has proved to constrain age and distance much more than the raw (observed) photometry (e.g. Bonatto & Bica 2010).

4.2. Colour-Magnitude Diagrams

CMDs built with the raw photometry of the present objects are shown in the top panels of Figs. 3, 4, 6 and 11. For qualitative comparison, CMDs extracted from equal-area comparison fields are shown in the middle panels. The decontamination itself is based on as large as possible field areas. Finally, the decontaminated CMDs are shown in the bottom panels, together with the respective CM filters.

Fundamental parameters (Table 2) are derived by means of the constraints provided by the field-decontaminated CMD morphologies combining the MS and PMS distributions. Historically, different approaches have been used to extract astrophysical parameters from isochrone fits. A review of these methods is given by Naylor & Jeffries (2006). In the present cases fits are matched *by eye*, taking the combined MS and PMS stellar distribution as constraint. Throughout the paper we use Padova isochrones with solar metallicity (Z=0.0019) [5] (Bressan et al. 2012) computed for the VISTA Z, Y, J, H and K_S filters. The derived fundamental parameters are given in Table 2, where we also provide the Galactocentric distance (R_{GC}), which is based on the derived value of the Sun's distance to the Galactic center $R_\odot$=7.2 kpc, computed by means of Globular clusters (Bica et al. 2006). We obtained $d_\odot$=1.78±0.1 kpc for the NGC 6357 complex based on the individual determinations for Pismis 24, BDS 101, ESO 392-SC 11 and VVV CL167 (Table 2).

4.2.1. Pismis 24

The decontaminated CMD of Pismis 24 (Fig. 3) presents a relatively vertical populous MS. It has a large population of red faint stars belonging to the PMS, making it a rather massive object in the sample. This cluster contains 12 known massive stars, three of them (Pis24-1NE, Pis24-1SW and Pismis 24-17) with ∼100 $M_\odot$ each (Maíz Apellániz et al. 2007). These stars are absent in 2MASS and are saturated in VVV. Consequently, they do not appear in our CMDs. There is a debate in the literature on the distance of Pismis 24, and published estimates range from 1.0 to 3.0 kpc. We fitted a set of Padova isochrones (0.2, 1, 3 and 5 Myr)

[5] http://stev.oapd.inaf.it/cgi-bin/cmd

Table 2. Derived fundamental parameters for the star clusters towards NGC 6357.

Cluster	A_V (mag)	Age (Myr)	$d_\odot$ (kpc)	R_{GC} (kpc)
(1)	(2)	(3)	(4)	(5)
Pismis 24	5.87±0.06	5±2	2.0±0.1	5.3±0.1
BDS 101	6.57±0.06	5±2	1.7±0.1	5.6±0.1
ESO 392-SC 11	6.69±0.06	5±2	1.9±0.1	5.4±0.1
VVV CL164	15.9±0.09	$(5 \pm 2) \times 10^3$	1.4±0.1	5.9±0.1
VVV CL167	4.94±0.06	9±2	1.6±0.1	5.6±0.1

Notes. Table Notes. Col. 2: A_V absorption in the cluster central region. Col. 3: age, from VVV photometry. Col. 4: distance to the Sun. Col. 5: R_{GC} distance of the object to the Galactic center.

(Fig. 3) leading to $E(J-K_S)$ = 1.01±0.01 ($E(B-V)$ = 1.75±0.10 or A_V = 5.87 ± 0.06). The observed and absolute distance moduli are $(m-M)_J$ = 13.20 ± 0.10 and $(m-M)_O$ = 11.50 ± 0.10, respectively, and $d_\odot$ = 2.0 ± 0.1 kpc. We estimated the mass of the PMS population of Pismis 24 by counting the number of PMS stars and multiplying it by a mean PMS stellar mass. We obtained 153 $M_\odot$. For the mean PMS stellar mass, we assumed an initial mass function of Kroupa (2001) between 0.08 and 7 $M_\odot$, which results in a mean mass of 0.6 $M_\odot$ (Bonatto & Bica 2010). For the MS stars in Fig. 3 the sum of the stellar masses is 80 $M_\odot$. Finally, we added the three saturated supermassive stars not included in the VVV photometry, totalling 533±50 $M_\odot$. We conclude that Pismis 24 is not an extremely massive cluster, having an intermediate mass which is mostly stocked in its massive stars.

4.2.2. BDS 101

BDS 101 is a compact cluster. Differently from Pismis 24 its CMD (Fig 3) shows a poorly-populated MS and a rich PMS. The single star that occupies the MS is an O5[6] star. We fitted a set of Padova isochrones (0.2, 1, 3, 5 and 7 Myr) (Fig. 3) leading to $E(J-K_S)$ = 1.13 ± 0.01 ($E(B-V)$ = 1.95 ± 0.10 or A_V = 6.57 ± 0.06). The observed and absolute distance moduli are $(m-M)_J$ = 13.0 ± 0.10 and $(m-M)_O$ = 11.09 ± 0.10, respectively, and $d_\odot$ = 1.66 ± 0.09 kpc. The computed parameters are consistent with those of Pismis 24, indicating that BDS 101 is also embedded in the NGC 6357 complex. The total mass estimate for BDS 101 is 106±10 $M_\odot$. Although a prominent cluster, it is not massive.

4.2.3. VVV CL167

We find that this cluster contains the WR star WR 93 (van der Hucht 2001). Historically, this star has been considered a likely member of Pismis-24 (Massey et al. 2001). WR stars usually have masses in the range 10-25 $M_\odot$, and present strong, broad emission lines of He and N (WN) or He, C and O (WC) (Meynet & Maeder 2005). Recently, clusters containing WR stars were studied with VVV (Chené et al. 2012). We point out that WR 93 is located too far (∼5′ West) from Pismis 24. The image (Fig. 2) and the CMD (Fig. 4) indicate a star cluster surrounding WR 93. We identify very few PMS stars in the CMD (Fig. 4). We adopted as best fit a Padova isochrone of 9 Myr (Fig. 4) that produces $E(J-K_S)$ = 0.85 ± 0.01 ($E(B-V)$ = 1.47 ± 0.10 or A_V = 4.94 ± 0.06). We get the observed and absolute distance moduli $(m-M)_J$ = 12.50 ± 0.10 and $(m-M)_O$ = 11.07 ± 0.10, respectively. The distance to the Sun is $d_\odot$ = 1.6 ± 0.1 kpc. In

[6] SIMBAD

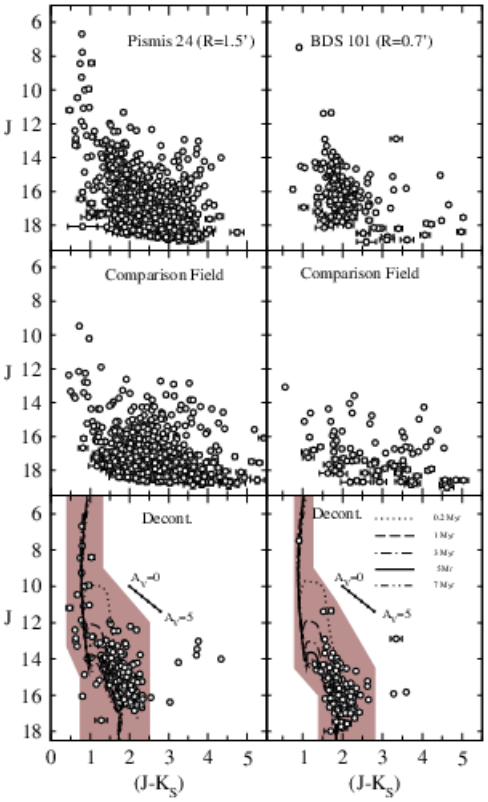

Fig. 3. Top left panel: Jx(J-K_S) CMDs of Pismis 24 showing the observed photometry for representative cluster and field regions. Middle left panel: equal-area extraction from the comparison field. Bottom left panel: The decontaminated CMDs fitted with Padova isochrones 0.2, 1, 3, 5 and 7 Myr, together with the Colour-Magnitude filter (brown polygon) used to isolate the MS and PMS stars. Right panels: the same for BDS 101. Reddening vector for A_v=0−5 mag is shown.

the colour-colour diagram (Fig. 5) the star WR 93 shows K_S-excess. A similar K_S-excess was observed for massive stars in the ∼ 14 Myr open cluster NGC 4755 (Bonatto et al. 2006a). The CMD of VVV CL-167 contains essentially only MS stars and WR 93. We obtain a cluster mass of 50±5 $M_\odot$. The cluster age and mass point to a dynamically evolved cluster.

4.2.4. VVV CL164 - a projected OC next to the complex

The decontaminated CMDs Jx(J-H)and Jx(J-K_S) are shown in the bottom panels of Fig. 6. We also include the CM filter on the Jx(J-H) decontaminated CMD. The remaining stars popu-

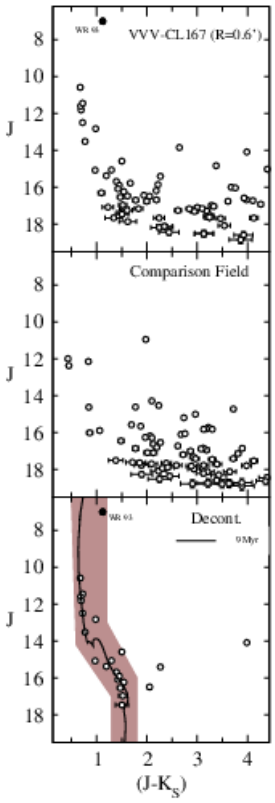

Fig. 4. Top panel: observed Jx(J-K$_S$) CMD of the region R¡0.6′ of VVV CL167. Middle left panel: equal-area extraction from the comparison field. Bottom panel: the decontaminated CMD best-fit Padova isochrone is 9 Myr (solid line) together with the CM filter (brown polygon). WR 93 is indicated.

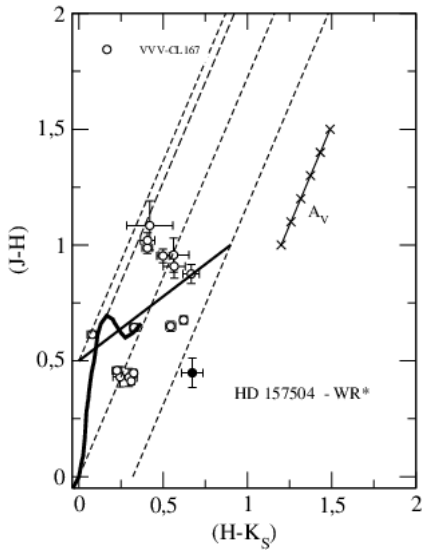

Fig. 5. Colour-colour diagram ((J-H)x(H-K$_S$)) of the decontaminated stars in VVV CL167. The continuous line represents the intrinsic distribution of spectral types and the continuous straight line indicates the undereddened locus of T Tauri stars. The reddening vector corresponds to A_V=5. Reddening directions for M5 giants, O3 and T Tauri stars are shown as dashed lines.

late sequences of typical intermediate-age open clusters, with evidence of a red clump and a turn-off (TO) in both colours. Blue stragglers appear to be present too. VVV CL164 presents relatively large errors at the TO level (J ∼18–19 mag). We matched a set of Padova isochrones (ages between 3 and 7 Gyr) and adopted 5 Gyr as the best solution (Fig. 6). We obtain $E(J-H) = 1.70 \pm 0.01$. ($E(B-V) = 4.73 \pm 0.15$ or $A_V = 15.9 \pm 0.1$). The A_V value is considerably larger than for the other clusters. The observed and absolute distance moduli are $(m-M)_J = 15.30 \pm 0.10$ and $(m-M)_O = 10.69 \pm 0.10$, respectively, resulting $d_\odot = 1.37 \pm 0.07$ kpc. We conclude that VVV CL164 is an intermediate-age cluster (5±2 Gyr) that is projected next to the NGC 6357 complex.

Contrasting with the young clusters in the complex, the CMD of VVV CL164 presents MS, TO and blue straggler stars, similar to those of M67 built with 2MASS data (Fig. 7). We estimated the mass of this relatively old open cluster by adding stars throughout the decontaminated CMD using the stellar masses for M 67 according to Bonatto & Bica (2003). We obtained ≈ 200 M$_\odot$ for VVV CL164.

4.3. Additional case: subclustering in Pismis 24?

The spatial distribution of YSOs in a cluster provides insights on the fragmentation processes leading to the formation of protostellar cores, evidence for triggered star formation and the subsequent dynamical evolution of the stars as they evolve from protostellar to the MS (Megeath et al. 2004).

In Fig. 8 we show the YSOs from Fang et al. (2012) in Pismis 24 area. Pismis 24 appears to have two close neighbours that are possible subclusters of YSOs. Blow up VVV images of these objects suggest clusters (Fig. 9). The stellar density excesses in the RDP (Sect. 4.5) of Pismis 24 produced by these two possible subclusters are indicated in Fig. 12. The formation of these young stars may have been influenced by winds from the nearby OB stars in the core of Pismis 24. A possible fate of the ensemble is merging with the more massive cluster (McMillan et al. 2007; Pang et al. 2013).

4.4. The EC ESO 392-SC 11 (AH 03 J1725-34.4)

Rahman et al. (2011a,b) have observed, in particular using GLIMPSE images and spectroscopy of luminous stars, far OB associations in the Galaxy which appear to be more massive than 10^4 $M_\odot$. In Fig. 10 we show a VVV K_s image of ESO 392-SC 11, where the compact cluster near the NW edge is BDS 101. The RDP of ESO 392-SC 11 appears to be rather flat (Fig. 13) like that of an association.

The decontaminated CMD Jx(J-K$_S$) is shown in the bottom panel of Fig. 11. We fitted a set of Padova isochrones (0.2, 1, 3 and 5 Myr) leading to $E(J-K_S) = 1.15 \pm 0.01$ ($E(B-V) = 1.99 \pm 0.10$ or $A_V = 6.69 \pm 0.06$). The observed and absolute distance moduli are $(m-M)_J = 13.3 \pm 0.10$ and $(m-M)_O = 11.36 \pm 0.10$, respectively, resulting in $d_\odot = 1.87 \pm 0.10$ kpc. This set of parameters shows that ESO 392-SC 11 is part of NGC 6357 complex, likewise Pismis 24 and BDS 101.

The off-Galaxy position of the Magellanic Clouds is suitable for size measurements of their stellar associations. Bica & Schmitt (1995) and Bica et al. (1999) measured size and position angle for 3226 associations in the Magellanic system (LMC, SMC, and Bridge). In the LMC, Lucke & Hodge (1970) reported diameters in the range 15-350 pc, while in the SMC, Hodge (1985) gave 20 to 140 pc. The smallest detected associations in the SMC (Bica & Schmitt 1995) and LMC (Bica et al. 1999)

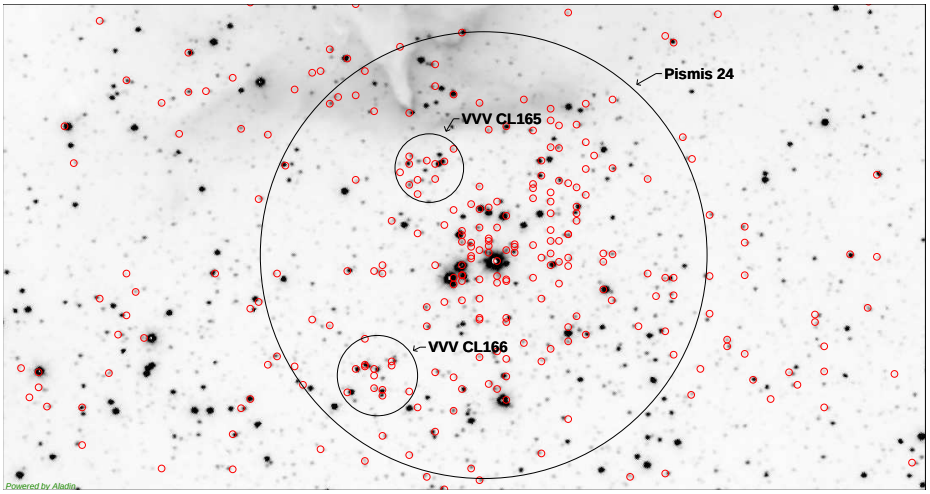

Fig. 8. $5' \times 3'$ VVV K_S image of Pismis 24 area (large circle). The probable subclusters VVV CL165 (top circle) and VVV CL166 (bottom circle) are indicated. The small red circles indicate YSOs (Fang et al. 2012). The shift between the stars in the VVV image and the YSOs from Fang catalog (2MASS data) is a consequence of the difference of angular resolution of each survey, 0.34″ and 2.0″ respectively. The black circle radius is given in Table 1.

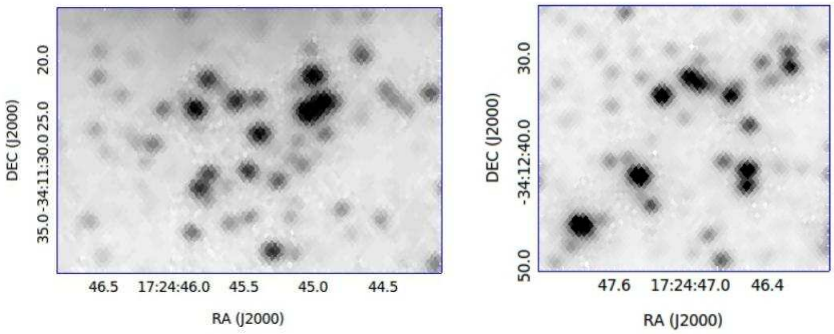

Fig. 9. K_S VVV blow up images of the probable subclusters located in Pismis 24. Left panel: VVV CL165. Right panel: VVV CL166.

have diameters of 5 and 7 pc, respectively, while the largest ones have typically 200 pc. The RDP radius of ESO 392-SC 11 is 3.3′ (Table 3). This value corresponds to a diameter of 2.6 pc, thus smaller than the lower limit of the associations in the Magellanic Clouds.

Some of the Magellanic Clouds associations were studied with HST reaching the PMS population. LH 95 in the LMC has a diameter about 40 pc and includes a series of PMS clusters (Gouliermis et al. 2007). The total mass of LH 95 with HST is 3000 $M_\odot$ (Da Rio et al. 2012). ESO 392-SC 11 in diagnostic diagrams (Sect. 5) involving structural parameters and mass behaves like a star cluster, rather than an association. As a cautionary remark, the Magellanic Clouds and the Galaxy have different tidal environments that should affect fragmentation of the molecular clouds.

Since ESO392-SC11 is made up of PMS stars and contains only a few MS stars, its association appearence will certainly change to one of a star cluster when more PMS stars evolve to the MS. Thus our results suggest that ESO392-SC11 is in a pre association stage. If the region loses gas and dust, then the system may be destabilized, later dynamically evolving to an association, after a star cluster phase.

4.5. Stellar density profiles

We use projected stellar RDPs, defined as the stellar number density around the cluster center, to derive structural parameters. Noise in the RDPs is minimised with CM filters, which exclude stars with colours that are not compatible with those of the cluster. Our group has shown that this filtering procedure considerably enhances the RDP contrast relative to the comparison field, especially in crowded fields (Bonatto & Bica 2007a). The CM filtered RDPs of the clusters are shown in Fig. 12.

Whenever possible, we fit a two-parameter King-like profile $\sigma(R)=\sigma_{bg}+\sigma_0/(1+(R/R_c)^2)$ (King 1966) adapted to star counts, where σ_0 and σ_{bg} are the central and residual stellar densities, and R_c is the core radius. The structural σ_0 and R_c parameters are derived from the fit, while σ_{bg} is previously measured in the comparison field and kept constant. The extent of the clusters (r_{RDP}) is defined as the radius where the RDP meets the field-star count level. The best-fit solutions and other results are condensed in Table 3. We point out that we are dealing with very young clusters (except VVV CL164). Thus we are not expecting relaxed systems, but interestingly the profiles even so describe the cluster RDP, such as the decontaminated profile of Pismis 24.

The absence of a central peak in the RDP of Pismis 24 (Fig. 12) is probably a consequence of the overshadowing produced by the bright stars on the surrounding faint members. The RDP

Table 3. Cluster structural parameters

Cluster	σ_0 (stars/$'^2$)	r_c ($'$)	R_c (pc)	σ_{bg} (stars/$'^2$)	r_{RDP} ($'$)	R_{RDP} (pc)
Pismis 24	85±26	0.76±0.20	0.44±0.11	31.9±0.9	3.2±0.3	1.9±0.2
BDS 101	157±40	0.48±0.21	0.23±0.04	22.1±1.0	2.3±0.2	1.1±0.1
ESO 392-SC 11	104±29	-	-	36±1.1	3.3±0.3	1.8±0.2
VVV CL167	24±14	-	-	6.8±0.4	2.3±0.2	1.1±0.1
VVV CL164	90±68	0.48±0.28	0.19±0.10	50.8±1.0	3.3±0.3	1.3±0.1

Notes. Col. 1: cluster designation. Col. 2: central density. Col. 3: core radius (arcmin). Col. 4: core radius (pc), assuming distances to the Sun in Table 2. Col. 5: background density. Col. 6: cluster RDP radius (arcmin). Col. 7: cluster RDP radius (pc).

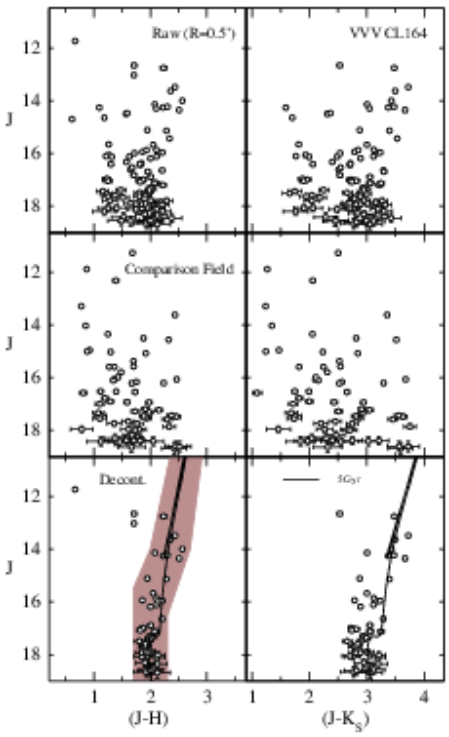

Fig. 6. Top left panel: observed Jx(J-H) CMD of the region R¡0.5 arcmin of VVV CL164. Middle left panel: equal-area extraction from the comparison field. Bottom left panel: the decontaminated CMD best-fit Padova isochrone (5 Gyr) together with the CM filter (brown polygon) used to isolate the MS and giants. Right panels: the same for Jx(J-K_S).

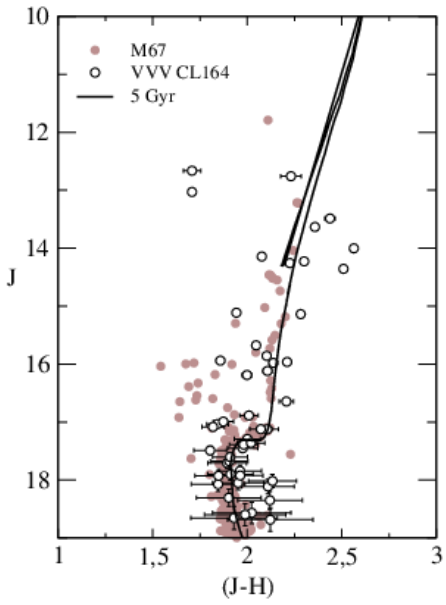

Fig. 7. Open cluster VVV CL164: comparison between the decontaminated Jx(J-H) CMD for the region R¡0.5 arcmin of VVV CL164 (empty circles) and the region R¡10 acrmin of M67 (filled circles). The best-fit to VVV CL164 is a Padova isochrone of 5 Gyr.

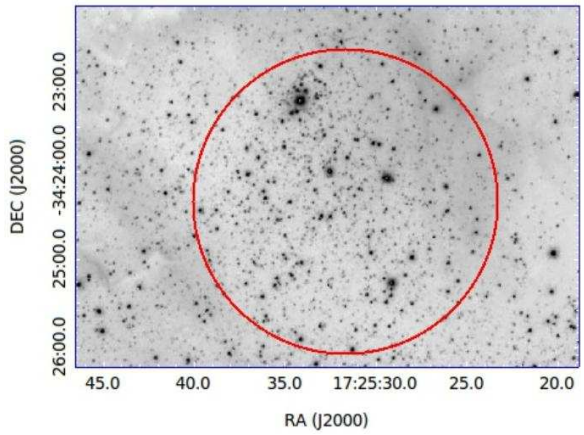

Fig. 10. K_S VVV image of ESO392-SC11. The circle indicates the object area. The compact cluster near the northern edge is BDS 101.

appears to present two excesses, supporting the existence of subclusters there (VVV CL165 and VVV CL166).

The irregular RDP of VVV CL167 could not be fitted by a King-like profile (Fig. 12). This suggests that VVV CL167 is a dynamically evolved cluster as a consequence of general mass loss, in particular winds from WR 93 and other less-massive stars that remove the interstellar material in the cluster (Tutukov 1978; Goodwin & Bastian 2006).

ESO 392-SC 11 has a peculiar profile (Fig. 13). We could not fit any King-profile. The superimposed contribution of the compact cluster BDS 101 could not be subtracted.

5. Object structure

We use structural parameters from Sect. 4.5 to investigate possible cluster evolutionary effects (Gieles & Portegies Zwart 2011; Saurin et al. 2012). Diagnostic diagrams for the dynamical evolution of star clusters have been built by our group in a series of papers (e.g. Bonatto & Bica 2009b; Bica et al. 2008; Bonatto & Bica 2010).

In Fig. 14 we show the estimated stellar mass compared to the extent RDP radius. For comparison purposes, we include a

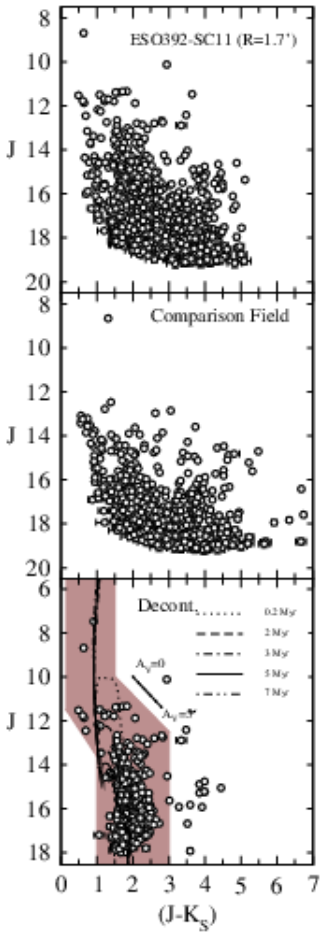

Fig. 11. Top panel: observed Jx(J-K$_S$) CMD of the region R¡1.7 arcmin of ESO 392-SC 11. Middle left panel: equal-area extraction from the comparison fields. Bottom panel: the decontaminated CMD together with the CM filter (brown polygon). MS and PMS isochrones are given.

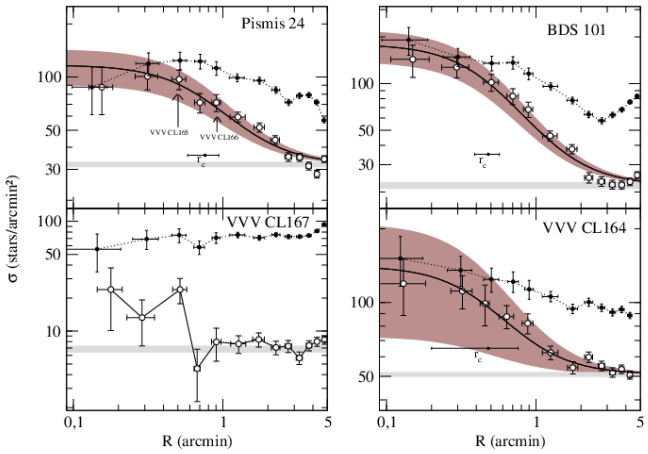

Fig. 12. Colour-magnitude filtered RDPs (empty circles). The dots represent the raw cluster profile. The empty circles show the cleaned profiles. The best King-like fit is shown, when possible. The 1σ fit uncertainty is represented by the heavy-shaded strip along the fit. The background level is the light-shaded region. The core radius (r$_c$) is indicated.

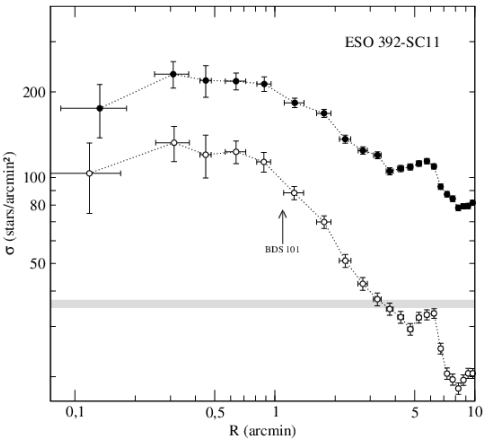

Fig. 13. Same as Fig. 12, for ESO 392-SC 11. The location of BDS 101 in the profile is indicated.

sample of nearby young clusters studied by our group following similar methods. The clusters are: NGC 2244 and NGC 2239 (Bonatto & Bica 2009b), NGC 6611 (Bonatto et al. 2006b), NGC 6823 (Bica et al. 2008), vdB 92 (Bonatto & Bica 2010), Pismis 5, vdB 80, NGC 1931 and BDSB 96 (Bonatto & Bica 2009c). We also include the large and populous associations Collinder 197 (Bonatto & Bica 2010), Bochum 1 (Bica et al. 2008), and Trumpler 37 (Saurin et al. 2012). In addition, we show LH 95, a massive LMC association studied with HST (Da Rio et al. 2012). The general behaviour of the clusters and associations appears to present a flattening effect, in the sense that associations tend to inflate while keeping large masses. The clusters in NGC 6357 present low to intermediate integrated stellar masses, but they are systematically smaller than the comparison clusters. Since they are located in the Sagittarius Arm, they are possibly affected by tidal effects, even at the phase of cloud fragmentation.

Another way of investigating this issue is by comparing the cluster radius (R_{RDP}) with the half-starcount radius (R_{hSC}). The latter is equivalent to the half-light radius usually used in star clusters studies in the outer parts of the Galaxy (e.g. Belokurov et al. 2009). The results are shown in Fig. 15, where again we use the same comparison clusters and associations (except LH 95) as in Fig. 14. The comparison clusters follow a power-law scaling relation for R_{RDP} and R_{hSC}. Again, the associations Collinder 197, Bochum 1 and Trumpler 37 appear to be inflated at the outskirts, when compared to the cluster scaling relation. The clusters in NGC 6357 are quite small when compared to the young reference clusters (Fig. 14). Note that ESO 392-SC11 (Fig. 13) lies in a similar locus as Pismis 24 (Fig. 14), thus implying a cluster behaviour.

6. Discussion and Conclusions

We studied the NGC 6357 star-forming complex with VVV photometry. The main focus of the present study are seven stellar clusters in the area. Pismis 24 is a relatively populous EC, with a developed MS and PMS. BDS 101 is compact with a CMD dominated by PMS stars. The EC VVV CL167 includes a WR star and is significantly older than Pismis 24 and BDS 101. VVV CL165 and VVV CL166 appear to be subclusters related

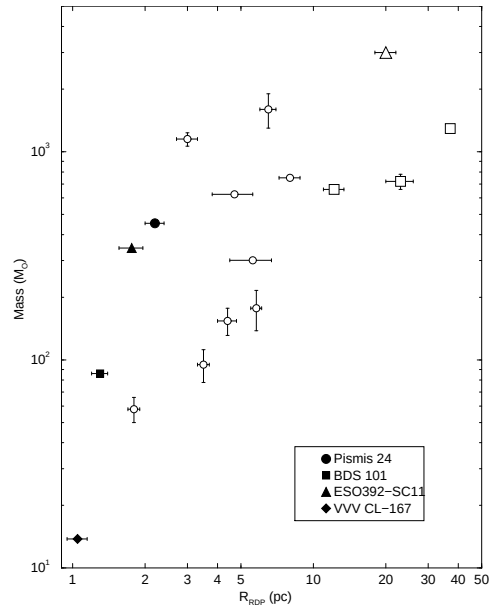

Fig. 14. Cluster or association mass × extent RDP radius. Open circles: comparison cluster sample; Open squares: associations or evolving associations; Open triangle: the LMC association LH 95. The present sample is indicated.

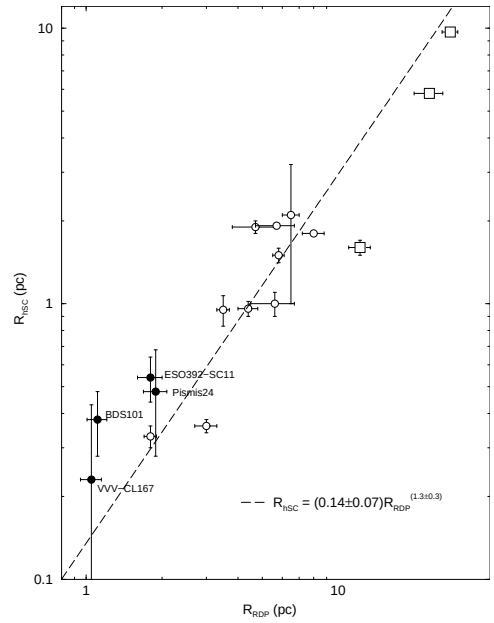

Fig. 15. The distribution of the half-starcount radius × extent radius. Symbols as in Fig. 14.

to Pismis 24. ESO392-SC11 is an interesting object, probably in a pre-association stage.

VVV CL164 to VVV CL167 were discovered in the present paper. From the clusters belonging to the complex (Pismis 24, BDS 101, ESO 392-SC 11 and VVV CL167) we derived a mean distance of $d_\odot$=1.78±0.1 kpc to NGC 6357. We also detected an open cluster of intermediate age (VVV CL164) projected next to the complex. Evidence is found that these clusters in NGC 6357 are small as compared to nearby embedded clusters. The NGC 6357 complex, now with several analysed ECs, resembles more its neighbouring complex NGC 6334 (Feigelson et al. 2009; Russeil et al. 2012, 2013).

In the cluster mass calculations (Sect. 4.2) we considered stars in the decontaminated area (corresponding to the radii given in column 6 of Table 1). Pismis 24 and ESO 392-SC 11 have intermediate masses, while the other clusters in NGC 6357 have low masses. Probably VVV CL167 is unstable and will lose additional gas mass in the coming Myrs (Bastian & Goodwin 2006).

In some aspects, the NGC 6357 complex emulates a star-forming dwarf galaxy, in the sense that besides a rich content of interstellar features it hosts embedded clusters pointing to at least two stellar generation events.

Acknowledgements. We thank the referee for important comments and suggestions. We acknowledge support from the Brazilian Institution CNPq. We gratefully acknowledge use of data from the ESO Public Survey programme ID 179.B-2002 taken with the VISTA telescope, data products from the Cambridge Astronomical Survey Unit. R.K.S. acknowledges support from CNPq/Brazil through projects 310636/2013-2 and 481468/2013-7. We acknowledge use of the VizieR Catalogue Service operated at the CDS, Strasbourg, France. This publication makes use of data products from the Two Micron All Sky Survey, which is a joint project of the University of Massachusetts and the Infrared Processing and Analysis Centre/California Institute of Technology, funded by the National Aeronautics and Space Administration and the National Science Foundation.

References

Archinal, B. A. & Hynes, S. J. 2003, Star clusters
Bastian, N. & Goodwin, S. P. 2006, MNRAS, 369, L9
Belokurov, V., Walker, M. G., Evans, N. W., et al. 2009, MNRAS, 397, 1748
Bica, E., Bonatto, C., Barbuy, B., & Ortolani, S. 2006, A&A, 450, 105
Bica, E., Bonatto, C., & Dutra, C. M. 2008, A&A, 489, 1129
Bica, E., Dutra, C. M., Soares, J., & Barbuy, B. 2003, A&A, 404, 223
Bica, E. L. D. & Schmitt, H. R. 1995, ApJS, 101, 41
Bica, E. L. D., Schmitt, H. R., Dutra, C. M., & Oliveira, H. L. 1999, AJ, 117, 238
Bohigas, J., Tapia, M., Roth, M., & Ruiz, M. T. 2004, AJ, 127, 2826
Bonatto, C. & Bica, E. 2003, A&A, 405, 525
Bonatto, C. & Bica, E. 2007a, A&A, 473, 445
Bonatto, C. & Bica, E. 2007b, MNRAS, 377, 1301
Bonatto, C. & Bica, E. 2009a, MNRAS, 392, 483
Bonatto, C. & Bica, E. 2009b, MNRAS, 394, 2127
Bonatto, C. & Bica, E. 2009c, MNRAS, 397, 1915
Bonatto, C. & Bica, E. 2010, A&A, 516, A81
Bonatto, C., Bica, E., & Lima, E. F. 2012a, MNRAS, 420, 352
Bonatto, C., Bica, E., Ortolani, S., & Barbuy, B. 2006a, A&A, 453, 121
Bonatto, C., Lima, E. F., & Bica, E. 2012b, A&A, 540, A137
Bonatto, C., Santos, Jr., J. F. C., & Bica, E. 2006b, A&A, 445, 567
Borissova, J., Chene, A. N., Ramirez Alegra, S., et al. 2014, submitted for publication
Bressan, A., Marigo, P., Girardi, L., et al. 2012, MNRAS, 427, 127
Camargo, D., Bonatto, C., & Bica, E. 2011, MNRAS, 416, 1522
Cappa, C. E., Barbá, R., Duronea, N. U., et al. 2011, MNRAS, 415, 2844
Carvalho, L., Saurin, T. A., Bica, E., Bonatto, C., & Schmidt, A. A. 2008, A&A, 485, 71
Chené, A.-N., Borissova, J., Clarke, J. R. A., et al. 2012, A&A, 545, A54
Conti, P. S. & Vacca, W. D. 1990, AJ, 100, 431
Da Rio, N., Gouliermis, D. A., Rochau, B., et al. 2012, MNRAS, 422, 3356
Damke, G., Barbá, R., & Morrell, N. I. 2006, in Revista Mexicana de Astronomia y Astrofisica, vol. 27, Vol. 26, Revista Mexicana de Astronomia y Astrofisica Conference Series, 180
Dias, W. S., Alessi, B. S., Moitinho, A., & Lépine, J. R. D. 2002, A&A, 389, 871
Fang, M., van Boekel, R., King, R. R., et al. 2012, A&A, 539, A119
Feigelson, E. D., Martin, A. L., McNeill, C. J., Broos, P. S., & Garmire, G. P. 2009, AJ, 138, 227
Felli, M., Persi, P., Roth, M., et al. 1990, A&A, 232, 477
Friel, E. D. 1995, ARA&A, 33, 381
Gieles, M. & Portegies Zwart, S. F. 2011, MNRAS, 410, L6
Goodwin, S. P. & Bastian, N. 2006, MNRAS, 373, 752
Gouliermis, D. A., Henning, T., Brandner, W., et al. 2007, ApJ, 665, L27
Hodge, P. 1985, PASP, 97, 530
Irwin, M. J., Lewis, J., Hodgkin, S., et al. 2004, in Society of Photo-Optical Instrumentation Engineers (SPIE) Conference Series, Vol. 5493, Optimizing Scientific Return for Astronomy through Information Technologies, ed. P. J. Quinn & A. Bridger, 411–422
King, I. R. 1966, AJ, 71, 64

Kroupa, P. 2001, MNRAS, 322, 231
Lada, C. J. & Lada, E. A. 2003, ARA&A, 41, 57
Lauberts, A. 1982, ESO/Uppsala survey of the ESO(B) atlas
Leisawitz, D., Bash, F. N., & Thaddeus, P. 1989, ApJS, 70, 731
Lortet, M. C., Testor, G., & Niemela, V. 1984, A&A, 140, 24
Lucke, P. B. & Hodge, P. W. 1970, AJ, 75, 171
Maíz Apellániz, J., Walborn, N. R., Morrell, N. I., Niemela, V. S., & Nelan, E. P. 2007, ApJ, 660, 1480
Massey, P., DeGioia-Eastwood, K., & Waterhouse, E. 2001, AJ, 121, 1050
McMillan, S. L. W., Vesperini, E., & Portegies Zwart, S. F. 2007, ApJ, 655, L45
Megeath, S. T., Allen, L. E., Gutermuth, R. A., et al. 2004, ApJS, 154, 367
Meynet, G. & Maeder, A. 2005, A&A, 429, 581
Minniti, D., Lucas, P. W., Emerson, J. P., et al. 2010, New A, 15, 433
Moffat, A. F. J. & Vogt, N. 1973, A&AS, 10, 135
Moisés, A. P., Damineli, A., Figuerêdo, E., et al. 2011, MNRAS, 411, 705
Naylor, T. & Jeffries, R. D. 2006, MNRAS, 373, 1251
Neckel, T. 1978, A&A, 69, 51
Neckel, T. 1984, A&A, 137, 58
Pang, X., Grebel, E. K., Allison, R. J., et al. 2013, ApJ, 764, 73
Persi, P., Ferrari-Toniolo, M., Roth, M., & Tapia, M. 1986, A&A, 170, 97
Rahman, M., Matzner, C., & Moon, D.-S. 2011a, ApJ, 728, L37
Rahman, M., Moon, D.-S., & Matzner, C. D. 2011b, ApJ, 743, L28
Russeil, D., Schneider, N., Anderson, L. D., et al. 2013, A&A, 554, A42
Russeil, D., Zavagno, A., Adami, C., et al. 2012, A&A, 538, A142
Russeil, D., Zavagno, A., Motte, F., et al. 2010, A&A, 515, A55
Saito, R. K., Hempel, M., Minniti, D., et al. 2012, A&A, 537, A107
Saurin, T. A., Bica, E., & Bonatto, C. 2010, MNRAS, 407, 133
Saurin, T. A., Bica, E., & Bonatto, C. 2012, MNRAS, 421, 3206
Skrutskie, M. F., Cutri, R. M., Stiening, R., et al. 2006, AJ, 131, 1163
Tutukov, A. V. 1978, A&A, 70, 57
van der Hucht, K. A. 2001, New A Rev., 45, 135
Walborn, N. R., Howarth, I. D., Lennon, D. J., et al. 2002, AJ, 123, 2754
Wang, J., Townsley, L. K., Feigelson, E. D., et al. 2007, ApJS, 168, 100
Wilson, T. L., Mezger, P. G., Gardner, F. F., & Milne, D. K. 1970, A&A, 6, 364